Water Research 276 (2025) 123249

Contents lists available at ScienceDirect

Water Research

journal homepage: www.elsevier.com/locate/watres

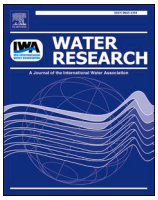

Exploring carbon dynamics in a slow sand filter using stable isotopes

Bayan Khojah [a,*], Salima Sadeghi [a], Lubos Polerecky [a], Jack J. Middelburg [a], Dick van Oevelen [b], Marcel T.J. van der Meer [c], Thilo Behrends [a]

[a] Department of Earth Sciences, Utrecht University, Princetonlaan 8a, Utrecht 3584 CB, the Netherlands
[b] Department of Estuarine and Delta Systems, NIOZ Royal Netherlands Institute for Sea Research, Korringaweg 7, Yerseke 4401 NT, the Netherlands
[c] Department of Marine Microbiology & Biogeochemistry, NIOZ Royal Netherlands Institute for Sea Research, Landsdiep 4, 't Horntje (Texel), 1797 SZ, the Netherlands

ARTICLE INFO

Keywords:
Biofiltration
Biological activity
Carbon isotope
Drinking water production
Organic matter removal

ABSTRACT

Slow sand filtration (SSF) is one of the oldest biofiltration methods for reducing pathogens and organic matter (OM) in water. Due to its efficiency, affordability, and operational simplicity, SSF remains a widely used approach for producing biologically stable drinking water. Although biological activity plays a role in the removal of OM during SSF, its contribution is poorly constrained. Here, we explored the utility of stable isotopes for investigating this role quantitatively on the scale of an operational filter. First, by combining measurements of concentrations and natural isotopic composition in relevant carbon pools (dissolved and solid, organic and inorganic), we found evidence for OM removal through both retention and subsequent mineralization. However, their relative contributions could not be constrained due to insufficient precision and continuity of available data and incomplete knowledge about the relevant isotope fractionation factors. In the other approach, we therefore used laboratory incubations of SSF cores with ^{13}C-labeled glucose over 14 days and found rapid removal of the tracer by the biological community, exceeding the assimilable organic carbon loading rate of the operational filter by 18 times. The glucose removal was not limited to the upper part of the sand column, the schmutzdecke, but occurred throughout the entire sand column. Furthermore, the removal was dominated by bacterial uptake over mineralization, with a substantial part likely retained as carbon reserves. The residence time of the tracer exceeded the duration of the experiment, hampering our ability to estimate the rate of OM mineralization. Analysis of the meiofauna indicated that grazing and/or predation constitutes only a minor sink for the bacterial biomass in the studied filter. Overall, this study illustrates the potential of stable isotopes for studying biological processes in SSF systems, including OM removal under diverse conditions, maturation of new or recently cleaned filters, or interactions within the endogenous biological community. To fully utilize this potential, future work should employ isotope labeling experiments with a longer duration, and consider more systematic and precise monitoring of the concentrations and isotopic composition in the relevant carbon pools.

Abbreviations

SSF	slow sand filtration
OM	organic matter
EPS	extracellular polymeric substances
SIL	stable isotope labeling
DOC	dissolved organic carbon
DIC	dissolved inorganic carbon
AOC	assimilable organic carbon
TSC	total solid carbon
SIC	solid inorganic carbon
SOC	solid organic carbon
BAC	bacteria
MEI	meiofauna
PLFA	phospholipid-derived fatty acids
IRMS	isotope ratio mass spectrometer

1. Introduction

Slow sand filtration (SSF) is a widely used water treatment method due to its efficiency, affordability, and operational simplicity. SSF can effectively reduce organic matter and pathogens to safe levels, resulting in a desirable degree of biological stability of the produced drinking water (Collins et al., 1992; Hijnen et al., 2004; Seeger et al., 2016). As

* Corresponding author.
E-mail address: B.a.a.khojah@uu.nl (B. Khojah).

https://doi.org/10.1016/j.watres.2025.123249
Received 5 July 2024; Received in revised form 4 February 2025; Accepted 5 February 2025
Available online 6 February 2025

revealed by numerous studies, key filtration mechanisms behind SSF include physical, chemical, and biological processes (Haig et al., 2015a; Hidayah et al., 2018; Weber-Shirk and Chan, 2007). While the physicochemical processes include adsorption, attachment, and straining, the biofiltration capabilities derive from the activity of organisms inhabiting the filters (Hammes et al., 2011), which include archaea, bacteria, protozoa, small invertebrates (meiofauna) and larger invertebrates (macrofauna), as well as viruses and phages (Bai et al., 2023; Bichai et al., 2011; Bomo et al., 2004).

The importance of biological processes in the performance of SSF is well documented (Haig et al., 2011; Hendel et al., 2001). The key biological processes include (i) secretion of extracellular polymeric substances (EPS) by microbes in the top few centimeters of the sand column, which alters the surface properties of the sand particles and changes the permeability of the filter, leading to enhanced adsorption and attachment of contaminants (Lubarsky et al., 2022); (ii) uptake and mineralization of organic matter, where the labile organic carbon load is utilized by the microbial community in the sand filter and thus effectively removed (Campos et al., 2002); and (iii) predation by protozoa, meiofauna, and macrofauna, or inactivation by viruses and phages, which contributes to the removal of pathogens (Lloyd, 1973; Unger and Collins, 2008). Special attention had been given to the top few centimeters of the sand filter, called the 'schmutzdecke' (a "dirty layer"), which was considered the active biological layer (Maurya et al., 2020) and presumed to be essential for SSF functional operation (Ranjan and Prem, 2018). The time it takes for adequate biomass to build up in the schmutzdecke is called the ripening or maturation period, and this period can span up to several months until the filter is considered functional (Huisman and Wood, 1974). However, recent studies demonstrated that deeper sand layers also contribute to the filtration processes (Chan et al., 2018; Trikannad et al., 2023), challenging the earlier emphasis on the schmutzdecke. Thus, studying deeper layers is necessary to achieve a more complete understanding of SSF functionality.

Biological activity in a slow sand filter has been proposed to correlate with its purification performance (Hijnen et al., 2004). However, quantitative information about the biological activity and its role in the removal of organic matter through carbon assimilation, predation, and mineralization is scarce (Haig et al., 2011; Hammes et al., 2011). Currently, we lack information about (i) the contribution of mineralization through organic matter uptake and respiration to the removal of particulate (e.g., microbes and detritus) and dissolved (labile as well as recalcitrant) organic matter, (ii) the roles of the different biological compartments, including bacteria and meiofauna, in the removal of organic matter in SSF, and (iii) the vertical distribution of the biological activity, specifically the contribution of the schmutzdecke relative to the deeper parts of the sand column. These knowledge gaps exist due to the challenges encountered when constructing detailed carbon budgets in a slow sand filter, because the relevant carbon pools are usually very small or change very slowly. To overcome these challenges, new approaches need to be developed to better assess carbon dynamics in SSF.

Stable isotopes are a useful tool for studying the fate and fluxes of elements such as carbon and nitrogen between different pools within aquatic systems. One possible approach is based on studying natural-level isotope ratios, which vary among different pools due to preferential utilization of specific isotopes by biological and chemical processes. For instance, microbial biomass is often enriched in ^{13}C relative to the substrate it uses. This enrichment is attributed to the kinetic isotope effect during the decarboxylation of pyruvate, leading to the release of CO_2 that is depleted in ^{13}C relative to the substrate utilized. Accordingly, aerobic respiration preferentially releases ^{12}C into the inorganic pool leading to the residual organic matter being more enriched in ^{13}C (Ghashghaie et al., 2003; Lerch et al., 2011). These different mechanisms lead to predictable shifts in the carbon isotopic composition and can therefore aid in tracing carbon cycling pathways within the system (Wang et al., 2015). Another approach for studying biogeochemical processes that drive aquatic ecosystem dynamics is based on stable isotope labeling experiments, where stable isotopes are deliberately introduced into the studied system as tracers (Glibert et al., 2018). For example, ^{13}C isotopes have been used as tracers to investigate how organic carbon is utilized, transformed, and transferred among different components of the system (Middelburg et al., 2000; Miyatake et al., 2014), providing insights into the fate of contaminants (Fang et al., 2000) or trophic interactions within food webs (Bergamino et al., 2011), and to quantify production and consumption rates (Evrard et al., 2010; van Oevelen et al., 2006a, 2006b). Although stable isotope experiments have been previously employed in water treatment methods and environmental research (Bridgeman et al., 2014; Haig et al., 2015b; Maqbool et al., 2020; Poberžnik et al., 2012), they have not been applied in the context of SSF to explore the role of biological activity in the removal of organic matter. Since stable isotope labeling experiments help link the catabolism and anabolism in living organisms (Glibert et al., 2018), data generated during such experiments can serve as a good quantitative indicator of the biological activity in SSF (Haig et al., 2015b).

This study aimed to test the utility of stable isotopes for quantifying the biological activity in a slow sand filter from an operational SSF utility. First, we tested whether the contributions of biological uptake and mineralization to organic carbon removal could be derived by measuring the concentration and natural isotopic signatures of relevant carbon pools within the influent and effluent water and the sand column. Then, as a complementary approach, we performed a stable isotope labeling (SIL) experiment using ^{13}C-labeled glucose as a substrate to trace carbon transformations within the SSF column over a period of 14 days. We chose ^{13}C-glucose because it is a proxy for easily assimilable and biodegradable organic matter and can be incorporated into a wide range of phospholipid-derived fatty acids (PLFAs) (Webster et al., 2006). PLFAs are effective biomarkers because these cell membrane components are present in constant amounts in specific organisms, allowing for biomass calculations based on the concentrations of particular molecules (Boschker and Middelburg, 2002). Additionally, PLFAs have a rapid turnover and thus are representative of active living biomass rather than inactive organisms (Middelburg, 2014). Our general approach was based on previous SIL experiments conducted in marine intertidal sediments (Evrard et al., 2010; van Oevelen et al., 2006a, 2006b), which we adapted for lab-scale sand columns. The relevant carbon pools that we monitored included dissolved organic carbon (DOC), dissolved inorganic carbon (DIC), total solid carbon (TSC), solid inorganic carbon (SIC), bacteria (BAC), and small invertebrates such as worms and arachnids, which we refer to here as meiofauna (MEI).

2. Materials and methods

2.1. Sample collection

Sand columns and water samples were obtained from the Dutch drinking water company Waternet at their production site Weesperkarspel (Amsterdam, the Netherlands). At this location, seepage water from the Bethune polder is used as the main water source, which is first pretreated by coagulation and sedimentation and subsequently stored for 90 days in an uncovered reservoir. Prior to SSF, the reservoir water is treated by rapid sand filtration, ozone disinfection, softening, and activated carbon filtration. SSF is done at a vertical flow velocity of 0.35 m h^{-1} over an indoor sand bed with a surface area of 605 m^2 and a height of 1.3 m (see Supplementary Table S1 for additional operational details).

Our sampling started six months after the filter's schmutzdecke was cleaned by mechanically disturbing and flushing the top 2 cm sand layer and removing the suspended organic material. To test the approaches based on measuring carbon concentrations and assessing natural isotopic compositions, water samples from the SSF influent and effluent were collected on multiple occasions between December 2020 and June 2023 (Table 1). Due to access restrictions, water samples were collected

Table 1
Carbon concentrations and isotopic signatures in the influent and effluent of the slow sand filters obtained at the production site. September 2021 (SIL) refers to samples collected during the retrieval of sediment cores used in the SIL experiment. For these data, the influent values are shown as a mean value ± standard error (n=2). The rest of the data are shown as one measured value ± analytical error, when available. *Refers to effluent product collected from all sand filters at the production site.

Sampling period		DOC (mmol L^{-1})	δ^{13}C-DOC (‰)	DIC (mmol L^{-1})	δ^{13}C -DIC (‰)	AOC (µmol L^{-1})
December 2020 (Filter A)	Influent	0.384 ±0.02	-26.6 ±0.04	2.13 ±0.02	-6.99 ±0.01	N/A
	Effluent	0.327 ±0.02	-26.3 ±0.04	3.12 ±0.02	-7.23 ±0.01	N/A
September 2021 (Filter B)	Influent	0.253 ±0.01	-26.9 ±0.04	3.11 ±0.07	-6.47 ±0.14	N/A
	Effluent	0.210 ±0.01	-25.0 ±0.04	3.15 ±0.07	-7.51 ±0.14	N/A
September 2021 (SIL) (Filter B)	Influent	0.237 ±0.01	-24.9 ±0.50	2.45 ±0.03	-7.02 ±0.08	N/A
	Effluent	N/A	N/A	N/A	N/A	N/A
February 2023	Influent	N/A	N/A	N/A	N/A	2.24
	Effluent*	N/A	N/A	N/A	N/A	1.74
June 2023 (Filter C)	Influent	0.392 ±0.02	-30.0 ±0.02	3.38 ±0.06	-7.11 ±0.05	N/A
	Effluent	0.345 ±0.02	-29.1 ±0.02	3.33 ±0.06	-7.61 ±0.05	N/A

from three different slow sand filters but within the same water production site, referred to here as filters A, B, and C. Filters A and B were full-scale filters, while Filter C was a pilot-scale filter last cleaned three years before sampling. The sand columns used for the stable isotope labeling experiment were collected from filter B in September 2021, at the time when the filter was taken out of operation and drained. Sand columns were collected by inserting acrylic cores (inner diameter 10 cm, height 30 cm; Supplementary Fig. S1) into the sand bed until a depth of 20 cm. Thus, the sand column had a height of 20 cm and the remaining 10 cm above the sand was later filled with influent water. Subsequently, the cores were carefully capped to minimize disturbance to the sand column and transported to the laboratory at Utrecht University in a cool box for further analysis and experimentation.

2.2. Stable isotope labeling experiment

Twelve sand columns were filled with fresh SSF influent water, sealed, and a continuous percolation in the downward direction was started. The constant flow rate (60 ml min^{-1}, corresponding to the vertical water flow velocity of about 0.45 m h^{-1}) was achieved by using peristaltic pumps and platinum-cured silicone tubing. At all times, the bottom outlet was connected to the top inlet to recycle the percolated water (Fig. 1). After 16 h, 1 mL of ^{13}C-glucose solution (concentration 18.6 g glucose L^{-1}, ^{13}C atom fraction 99%; Cambridge Laboratories) was injected into each core, corresponding to 0.6 mmol of glucose-derived ^{13}C added per core. To ensure an even distribution of the isotope label throughout the column, injections were performed in five steps separated by 10–15 min, each containing 200 µL of the ^{13}C-glucose solution. Additionally, continuous circulation of the water at a flow rate of 0.45 m h^{-1}, corresponding to an average residence time of 20 min inside the sand column, was expected to exceed the glucose uptake rate. Therefore, we expect this approach has ensured homogeneous glucose distribution throughout the column. Although the continuous recycling does not accurately reflect the flow-through design implemented in SSF, it was necessary to keep the limited amount of added ^{13}C tracer inside the experimental system and thus allow mass balance calculations. Incubations were carried out in the dark at 18 °C to mimic the conditions of the full-scale SSF (Supplementary Table S1).

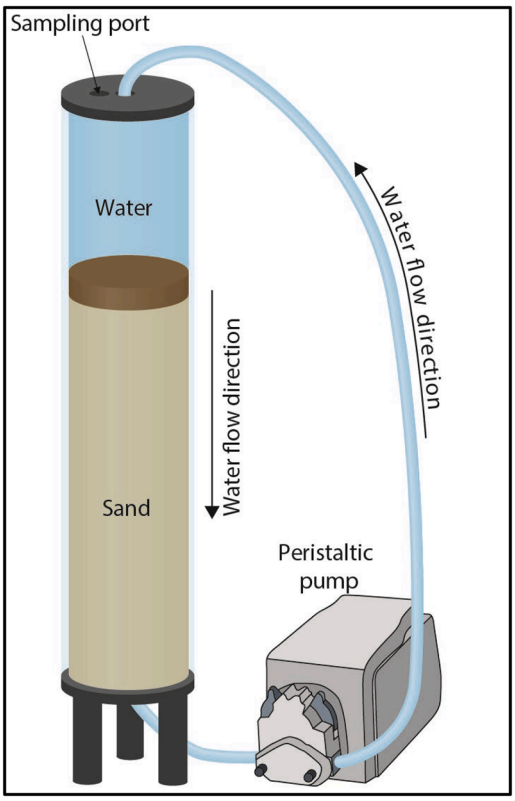

Fig. 1. A flow-through core used during the stable isotope labeling experiment.

To unravel the fate of the added ^{13}C-glucose, water and sand samples were collected at selected time points and preserved for the analyses of total C and ^{13}C content in the relevant carbon pools. During the first 6 h after label addition, overlying water samples were collected through a sampling port from two dedicated cores for the analysis of glucose, DIC, ^{13}C-DIC, DOC, and ^{13}C-DOC. For a more thorough analysis, water and sand samples were collected 6 h and 1, 2, 7, and 14 days after label addition. At each time point, duplicate cores were sacrificed. First, the cores were disconnected from the peristaltic pumps, and the overlying water was sampled for the analysis of DIC, ^{13}C-DIC, DOC, and ^{13}C-DOC. Then, the water was drained from the sand columns, and the sediment was sliced into three layers (0–2 cm, 2–5 cm, and 5–10 cm), homogenized by manual mixing, and prepared for the analysis of TSC, ^{13}C-TSC, SIC, ^{13}C-SIC, total C, and ^{13}C in PLFA (phospholipid-derived fatty acids) and total C and ^{13}C in meiofauna specimens. Two sand cores sacrificed at time point zero, i.e., without any contact with the ^{13}C-glucose, were used as background controls for the natural (unlabeled) isotopic composition. The natural ^{13}C content in the TSC pool was additionally determined from three other sand cores, two of which were percolated for 14 days without the injection of ^{13}C-glucose, while the third one was collected and sliced one week before the SIL experiment (Supplementary Table S2).

2.3. Analytical procedures

Water samples for the analysis of DOC and DIC concentrations and their isotopic signatures were filtered through 0.2 µm nylon filters. The DIC and ^{13}C-DIC samples were stored in gas-tight vials with no headspace. To stop the biological activity and ensure that no changes in the isotopic signatures occurred, the ^{13}C-DOC samples (20 mL) were poisoned with $ZnCl_2$ (10 µl of 50% w/v $ZnCl_2$ per milliliter of water sample) and stored in glass vials. The vials were heated to 550 °C for two hours before use to ensure that they were free of organic residues.

For the analysis of DIC and ^{13}C-DIC, 0.7 mL of water samples were

added through a septum using a syringe to closed vials containing 0.1 mL 85% H_3PO_4 and a helium-flushed headspace. The analysis was done using a Thermo Scientific GasBench II coupled with a Delta plus advantage isotope ratio mass spectrometer (IRMS). DOC concentrations were measured using a Shimadzu TOC-V analyzer (model CPH). ^{13}C-DOC was measured at KU Leuven, Belgium, using an Aurora 1030W TOC analyzer coupled to a Delta XP IRMS via gasbench and cryofocusing. Glucose concentrations were determined by an enzymatic assay (R-Biopharm) based on the production of NADPH quantified by UV/Vis spectrophotometry at 340 nm (Henniger and Mascaro, 1985). Assimilable organic carbon (AOC) was measured at Het Waterlaboratorium, the Netherlands, based on van der Kooij (1992). The values of the Langelier saturation index (LSI), a measure for calcium carbonate saturation, were provided by Waternet.

TSC and ^{13}C-TSC analyses were carried out on sand samples that were first freeze-dried and then ground using a ball mill grinder. Based on reports of calcite accumulation in SSF (Hammes et al., 2011), three sample pre-treatments were examined: (i) untreated sand, (ii) sand treated by standard decalcification, and (iii) sand washed with Milli-Q water (Supplementary Method S1). TSC and ^{13}C-TSC analyses were then carried out using a Thermo Scientific EA IsoLink CN analyzer coupled with a Delta V Advantage IRMS.

For the analysis of SIC and ^{13}C-SIC, freeze-dried and ground sand samples were placed in an exetainer vial, and the gas phase was replaced with helium by flushing for 5 min. Next, the samples were digested with 100% H_3PO_4 at 70 °C for 105 min. The analyses of the produced CO_2 were carried out using a Thermo Scientific GasBench II coupled with a Delta plus advantage IRMS. Since the samples analyzed for TSC, ^{13}C-TSC, SIC, and ^{13}C-SIC originated from the same homogenized sand slices, the corresponding amounts of solid organic carbon (SOC) and ^{13}C-SOC in the samples were calculated using the following mass balances: SOC = TSC – SIC and ^{13}C-SOC = ^{13}C-TSC – ^{13}C-SIC.

To extract the PLFA from the sand samples, a modified Bligh Dyer extraction method was used (Schouten et al., 2008) (Supplementary Method S2). Concentrations of individual fatty acids were quantified by Agilent gas chromatography (GC) equipped with a flame ionization detector (FID). For the measurement of the stable carbon isotopic composition of the individual fatty acids, Agilent GC single quad mass spectrometry for fatty acid identification and Thermo Scientific Delta V coupled to a Thermo Scientific Trace 1310 GC combustion isotope ratio monitoring MS (GC-C-IRMS) was used.

Meiofauna were extracted from the sand samples with a gradient centrifugation technique using colloidal silica polymer following a modified procedure by Somerfield and Warwick (2013) (Supplementary Method S3). The total C and ^{13}C contents were measured using a Thermo Scientific EA IsoLink CN analyzer coupled with Delta V advantage IRMS.

2.4. Data processing and analyses

Carbon contents in the studied pools were calculated from the concentrations measured in mol L^{-1} (for solutes) and wt% (for solids). When calculating the amounts of DIC and DOC in the porewater of the sand column, we assumed a porosity of 0.4 (Supplementary Table S1), whereas we additionally accounted for the overlying water volume when calculating these quantities in the cores used for the SIL experiment. The porosity was estimated based on the mass difference between water-saturated and dry sand (see Supplementary Method S4). When calculating the amounts of TSC, SIC, and SOC from the measured wt%, we assumed a dry sand density of 2.6 g cm^{-3}. The values were calculated separately per sand layer as well as per entire 20 cm sand column in the core. In the latter step, concentrations determined for the 5–10 cm layer were assumed to be representative for the entire part of the core below 5 cm. At the end, C pool sizes were converted to mol C m^{-2} by accounting for the cross-section of the experimental cores (78.5 cm^2; Supplementary Fig. S1).

Two alternative approaches were used to estimate the bacterial carbon concentrations from the measured PLFA concentrations (see Supplementary Method S5 for details). The first approach used weight-averaged concentrations of PLFAs with chain lengths below C19 and a conversion factor according to Leckie et al. (2004). The second approach followed the procedure described by Middelburg et al. (2000) using the concentrations of five bacterial-specific PLFAs (i14:0, i15:0, a15:0, i16:0, and 18:1 ω7c). Both methods introduce some uncertainty: the first one due to the possible inclusion of non-bacterial PLFA, and the second one due to the large conversion factor needed to go from the minor bacteria-specific PLFA to total cellular carbon content.

The isotopic composition in the studied carbon pools was quantified relative to the Vienna Pee Dee Belemnite (VPDB) standard and is presented in the delta notation: $\delta^{13}C\ (‰) = (\frac{R}{R_{VPDB}} - 1)\ 1000‰$, where R refers to the $^{13}C/^{12}C$ isotope ratio in the sample and $R_{VPDB} = 0.0111802$. The $\delta^{13}C$ values were subsequently combined with the measured C contents (in TSC, SIC, SOC, BAC, and MEI pools) to quantify the transfer of ^{13}C during the labeling experiment. Specifically, the amount of ^{13}C-glucose derived carbon incorporated into a particular pool during a time interval from 0 to t was calculated according to Polerecky et al. (2021). $\Delta^{13}C = x_S^E \cdot C$, where $x_S^E = (x - x_0)/(x_s - x_0)$ is the source-normalized ^{13}C excess atom fraction and C is the carbon content in the pool, both at time point t. In the expression for x_S^E, x is the ^{13}C atom fraction at time point t, calculated from the measured $\delta^{13}C$ permil-value according to $x = R/(1+R)$, where $R = (1 + \delta^{13}C/1000‰) \cdot R_{VPDB}$. Furthermore, x_0 and x_s are the ^{13}C atom fractions of the control (unlabeled) sample and ^{13}C-glucose ($x_s = 0.99$), respectively.

Statistical analyses involved fitting the TSC, SIC, and SOC data with a linear mixed model using depth and time as fixed factors and additionally considering the hierarchical structure of the data (i.e., nesting of depths within a core). The analyses were done in R (R Core Team, 2024) using the package nlme (Pinheiro et al., 2021), and the details are provided as Supplementary Materials. Quantities derived from replicate cores are reported as mean values ± standard error (SE) unless stated otherwise.

3. Results

3.1. Characterization of the dissolved and solid carbon pools

The concentration and isotopic composition of DOC in the influent and effluent of the slow sand filters at the water production site varied among the four sampling occasions (Table 1). The effluent had, however, consistently lower DOC concentrations (on average by 0.049 ± 0.006 mmol L^{-1}) and δ^{13}C-DOC values that reflect higher enrichment in ^{13}C (δ^{13}C-DOC increased by 1.03 ± 0.66 ‰) compared to the influent. In contrast, the DIC in the effluent was consistently more depleted in ^{13}C (δ^{13}C-DIC values decreased by 0.59 ± 0.33 ‰) compared to the influent, while DIC concentrations were either higher in the effluent or the difference was minimal and within the margin of analytical uncertainty. One measurement of AOC showed that AOC concentrations were roughly 100-fold lower than DOC concentrations and decreased by about 0.5 μmol L^{-1} between the influent and effluent. The Langelier saturation index (LSI) for the effluent was 0.36, indicating that the water was over-saturated with respect to calcite.

The total carbon pool within the 20 cm sand column was vastly (>99%) dominated by solid substances over porewater constituents DIC and DOC (Fig. 2). The total solid carbon (TSC) content varied considerably among the replicate cores, averaging at 56 ± 2 mol C m^{-2}. About 17% of this amount was contained in the schmutzdecke (top 2 cm), although the volume of this layer only comprises about 10% of the investigated sand column. This pattern was caused by about 2-fold greater TSC concentrations in the schmutzdecke (0.37 ± 0.03 wt%) compared to the deeper layers (0.20 ± 0.02 wt%) (Table 2). The TSC pool contained slightly more organic than inorganic carbon, and this relative proportion showed a significant vertical gradient within the

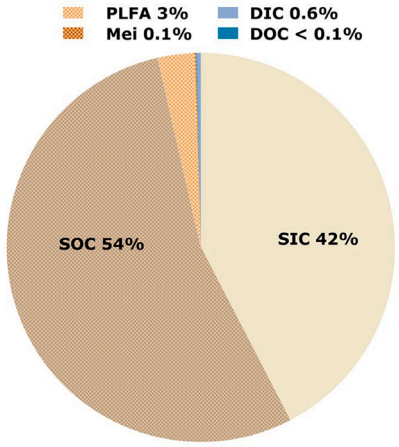

Carbon pool	Total carbon (mol m^{-2})	~δ^{13}C (‰)
DIC (dissolved inorganic C)	0.20 ± 0.002	-7.02 ± 0.08
DOC (dissolved organic C)	0.02 ± 0.001	-24.9 ± 0.50
SIC (solid inorganic C)	23.8 ± 1.65	-0.78 ± 0.33
SOC (solid organic C) inc. BAC and MEI	32.1 ± 2.80	-30.8 ± 2.45
BAC (bacteria)	1.73 ± 0.10	-27.9 ± 0.11
MEI (meiofauna size > 38 μm)	0.07	-25.9 ± 0.01
TSC (total solid C, SIC+SOC)	55.9 ± 2.03	-15.3 ± 2.11
TC (total C, TSC+DIC+DOC)	56.2 ± 2.03	

Fig. 2. Characteristics of the relevant carbon pools in the experimental sand columns. Values are normalized per area of a sand column with a height of 20 cm. The pie chart shows the relative contribution of each pool.

Table 2
Characteristics of the relevant carbon pools in the studied sand columns. Shown are values from different depth intervals within the columns. Values for concentrations of TSC, SIC, and SOC are given in weight percent and are based on n=12 replicate samples, whereas the δ^{13}C-TSC, δ^{13}C-SIC, and δ^{13}C-SOC values are based on duplicate samples (n=2).

Sampling period	Sand Depth	Total solid carbon (TSC) (wt %)	δ^{13}C -TSC (‰)	Solid Inorganic carbon (SIC) (wt%)	δ^{13}C-SIC[†] (‰)	Solid organic carbon (SOC)[‡] (wt %)	δ^{13}C-SOC[‡] (‰)
September 2021	0–2 cm	0.37 ± 0.03	-18.6 ± 1.69	0.12 ± 0.01	0.07 ± 0.25	0.25 ± 0.03	-26.7 ± 1.88
	2–5 cm	0.20 ± 0.02	-14.6 ± 1.20	0.07 ± 0.01	0.40 ± 0.25	0.12 ± 0.02	-29.7 ± 4.09
	5–10 cm	0.20 ± 0.01	-14.9 ± 2.36	0.09 ± 0.01	-1.12 ± 0.53	0.11 ± 0.01	-31.6[#]

[†] Determined using GasBench II-IRMS.
[‡] Estimated based on differences between TSC and SIC.
[#] Value derived from n=1 replicate sample.

sand column, with the solid organic carbon (SOC) fraction decreasing from about 67% in the schmutzdecke to 59% in the bottom 15 cm (Supplementary Fig. S2 and Supplementary statistical analyses 1). The average SOC fraction across the top 20 cm of the sand column was 57%, which translates to the SOC content of about 32 ± 3 mol C m^{-2}. Estimates of the carbon content in the bacterial and meiofaunal pools amounted to roughly 5% and 0.2% of the SOC pool, respectively.

δ^{13}C values in the SIC pool were about 0‰ throughout the sampled sand column, whereas in the TSC pool, δ^{13}C values were negative and reflected an increase in the relative abundance of ^{13}C with depth (from about –19‰ in the schmutzdecke to –15‰ in deeper layers). When combined with the carbon content data, this trend suggests that the SOC in the sand column has increased due to the retention of the input DOC pool. Specifically, by considering the observed vertical gradient in the relative fractions of SOC and SIC in the TSC pool (Supplementary Fig. S2), the observed value of δ^{13}C-SIC = 0‰, and assuming the δ^{13}C-SOC values to be in the range observed for the isotopic signature of the input DOC (between –30‰ and –25‰; Table 1), the predicted δ^{13}C-TSC values match well with the measured ones (Supplementary Fig. S3).

Average δ^{13}C values in the bacterial pool (corrected for fractionation as described by Monson and Hayes (1982) and Teece et al. (1999) and meiofaunal pool were around –25‰ and –26‰, respectively.

3.2. Stable isotope labeling experiment

Following the addition of ^{13}C-glucose into the experimental cores (0.6 mmol ^{13}C per core), glucose concentrations in the percolated water decreased approximately linearly ($R^2 = 0.91$, x-intercept = 4.6) over the first 4 h and fell below the detection limit of 0.002 mmol glucose L^{-1} after 5 h of incubation (Fig. 3A). The average rate of ^{13}C-glucose consumption, estimated using linear regression, was about 0.11 mmol ^{13}C h^{-1} per core. The addition and removal of ^{13}C-glucose was reflected in the isotopic signature of the total DOC pool, which was highly enriched in ^{13}C after 1 h of incubation (δ^{13}C > 2.5×10^5 ‰) and decreased rapidly within the first 6 h and then more gradually during the remainder of the experiment (Fig. 3B) because of preferential use of the added glucose relative to the remaining dissolved organic compounds. DOC concentrations did not change significantly during this time interval and remained at around 0.26 mmol L^{-1} (Supplementary Fig. S4). These latter values are, however, unreliable since they do not show the expected correlation with the concentrations of glucose. This discrepancy highlights the necessity of using complementary methods to accurately assess carbon uptake and ensure reliable experimental results. Consequently, we relied on glucose and δ^{13}C-DOC measurements to assess glucose uptake in this study.

^{13}C-glucose removal in the experimental cores was accompanied by a matching increase in δ^{13}C-DIC (Fig. 4), indicative of biological activity within the sand column and particularly of its rapid response to glucose

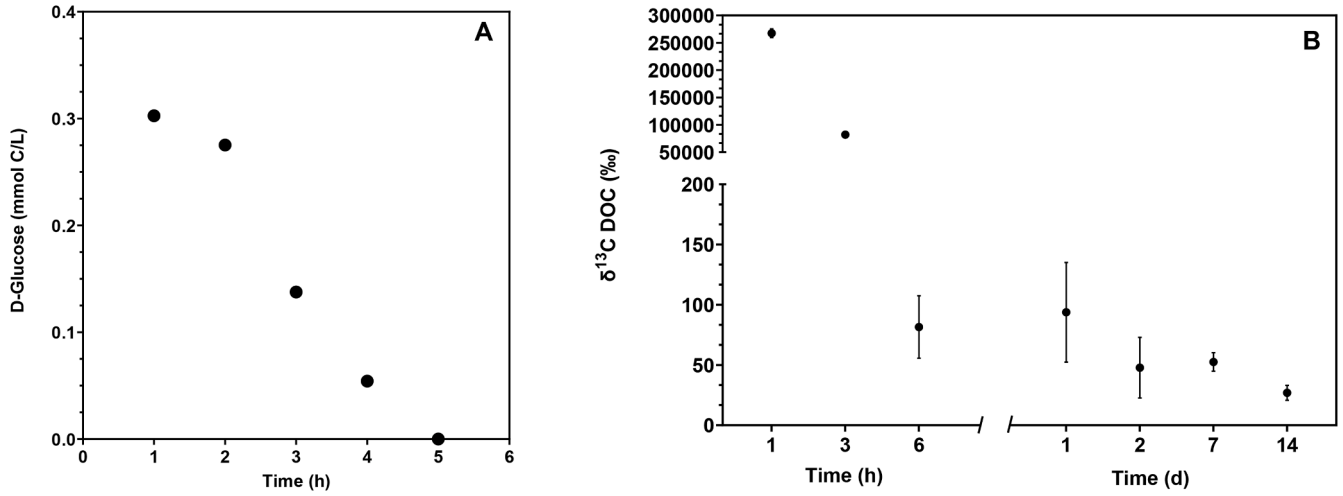

Fig. 3. Dynamics of the dissolved organic carbon pools in the cores during the stable isotope labeling experiment. (A) Concentrations of the added ^{13}C-glucose (n=1). (B) Isotopic composition of DOC (n=2). Time 0 refers to a time point before glucose was injected into the core. Note the cut in the x and y axes. Error bars represent the range between duplicate cores.

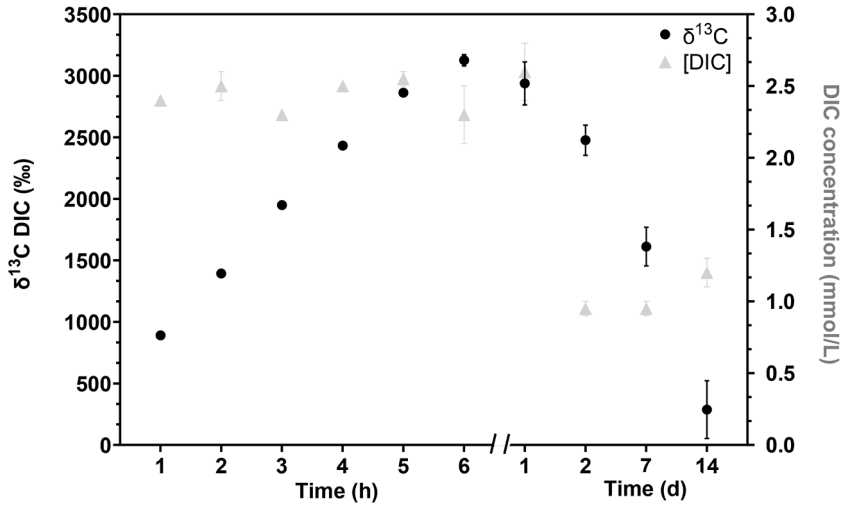

Fig. 4. Dynamics of the dissolved inorganic carbon pool in the cores during the stable isotope labeling experiment. Symbols represent the mean value (n=2), error bars represent the corresponding range. Some error bars appear missing because they are smaller than the size of the symbols.

addition. The δ^{13}C-DIC values first increased linearly (R^2 = 0.99), reaching above 3000‰ after 6 h of incubation, then gradually decreased over the following days and reached approximately 250‰ at 14 days. During the first 24 h, DIC concentrations remained approximately constant at 2.4 mmol L^{-1}, whereas they dropped to about 1 mmol L^{-1} on day 2, 7, 14. These latter values are, however, unreliable because the samples were stored for a few weeks before the analysis, during which CO_2 could have escaped from the sampling vials. A similar drop in DIC concentration between the samples taken from the initial influent water and those collected after two days was also observed in control columns that were percolated for 14 days without the addition of ^{13}C-glucose (Supplementary Table S3). The average rate of ^{13}C-DIC production after glucose addition during the initial 5 h, estimated using linear regression, was 0.013 mmol ^{13}C h^{-1} per core. This rate is about 8.5-fold lower than the glucose consumption rate, indicating that, during this time interval, only about 12% of ^{13}C-glucose removed within the sand column was mineralized to ^{13}C-DIC while the rest was transferred to the solid carbon pool.

Consistent with this expectation, a significant enrichment in ^{13}C was observed in the TSC pool, whose δ^{13}C-TSC values increased relative to those in the control cores on average by about 66‰ during 6 h of incubation (Fig. 5A). At this time point, we detected a significant ^{13}C enrichment in the SIC (Fig. 5D) pool as well (Supplementary statistical analyses 2), but the increase relative to controls was only by about 1‰. Combining the δ^{13}C values and carbon contents in the TSC and SIC pools, the calculated δ^{13}C values in the SOC pool (Fig. 5G) increased by about 110‰ during 6 h of incubation. For all three pools, the observed increases in δ^{13}C were similar for all depths in the sand column (Supplementary statistical analyses 2).

Although the δ^{13}C values in the TSC, SIC and SOC pools showed clear differences between the control samples and samples incubated for 6 h or more, no such differences were detectable for the ^{13}C contents calculated by combining the measured C contents and δ^{13}C values (Supplementary Fig. S5), which prevented us from using ^{13}C contents obtained in this way to directly estimate the amount of label transferred from ^{13}C-glucose to the solid carbon pools. We hypothesized that this lack of sensitivity was due to large differences in the C content among the sediment cores used in the SIL experiment (Fig. 5B, E, H). To test this hypothesis, we fitted the observed C contents with linear mixed models, considering `time' and `depth' as fixed factors and `core' as a random factor (see Supplementary statistical analyses 3 for details). These statistical analyses revealed that the effect of `time' was not significant (p =

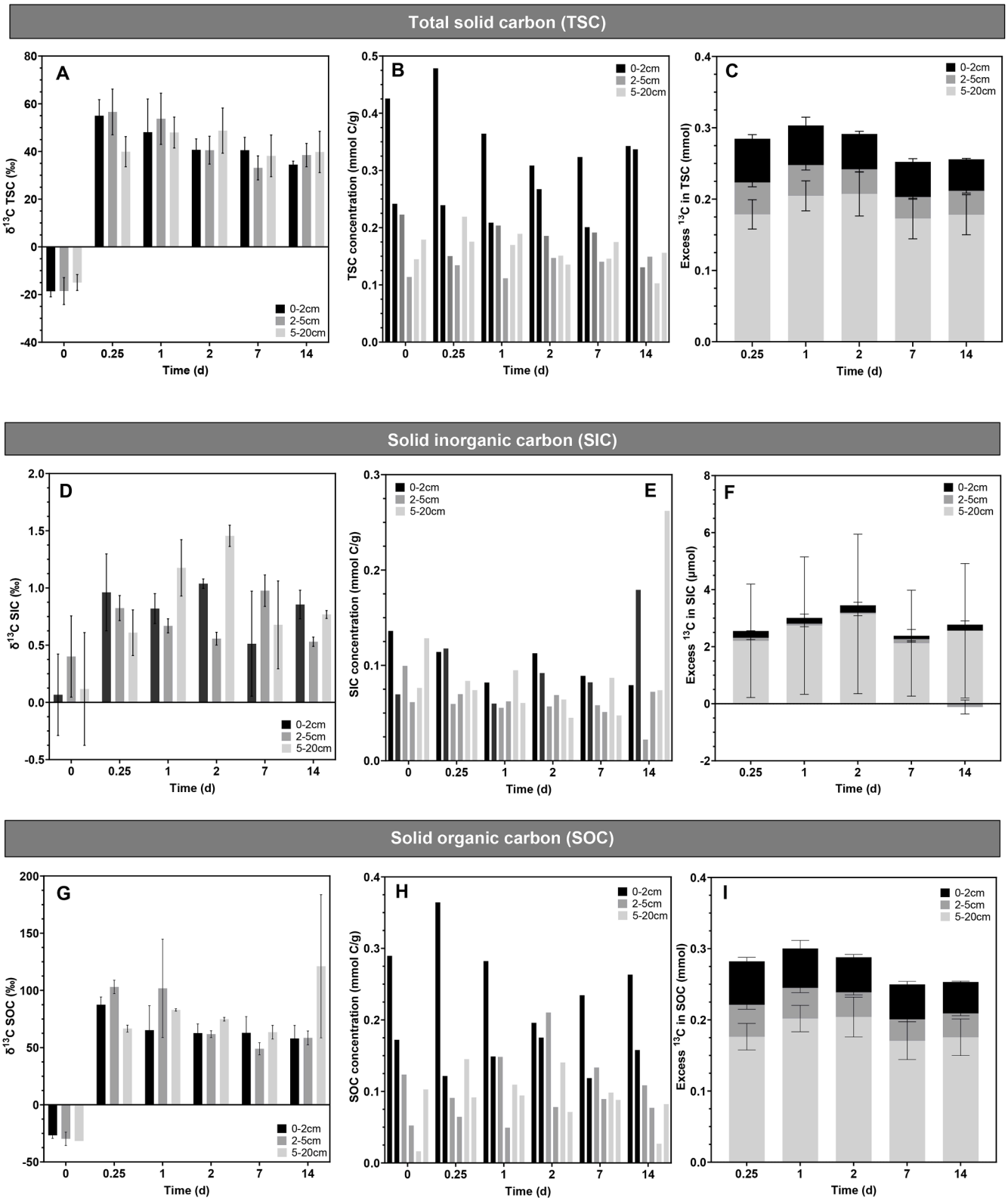

Fig. 5. Dynamics of the solid carbon pools in the cores during the stable isotope labeling experiment. TSC and SIC data are measured, while SOC data are calculated according to SOC = TSC – SIC and ^{13}C-SOC = ^{13}C-TSC – ^{13}C-SIC. (A,D,G) Average isotopic composition, expressed in δ^{13}C notation relative to VPDB. (B,E,H) Carbon concentrations. Values are shown separately for each sand column to highlight inter-core variations. (C,F,I) Calculated amounts of excess ^{13}C incorporated into the respective solid carbon pools per layer. Error bars, if present, represent the range based on duplicate cores.

0.051), confirming that inter-core differences were the key source of variability in the C contents observed throughout the SIL experiment. In contrast, the effect of `depth' was highly significant ($p < 0.0001$), with a roughly 1.8-fold greater C content in the schmutzdecke compared to the deeper sand layers. Based on these results, we averaged C contents over all time points, but separately for each depth, and calculated the amount of ^{13}C incorporated (i.e., excess ^{13}C) into the different solid carbon pools by combining the $\delta^{13}C$ values measured at each depth and time point with the corresponding time-averaged C content. A consequence of the C-content averaging, similar to van Oevelen et al. (2006a), is that the carbon dynamics in the SSF are evaluated on the ^{13}C dynamics only, which represent a good proxy for short-term carbon cycling.

The average amount of ^{13}C incorporated into the TSC pool was around 0.3 mmol ^{13}C per core (Fig. 5C), which is roughly 50% of the amount of glucose-derived ^{13}C added to each core. Due to the higher TSC concentration in the schmutzdecke, the concentration of ^{13}C that ended up in this layer was almost two-fold higher than in the lower parts of the sand columns. Considering the thickness of this layer, however, ^{13}C incorporated into the schmutzdecke comprised only 17% of the label incorporated per core. Although the amount of ^{13}C-TSC incorporated in the schmutzdecke appeared to decrease beyond 6 h (Fig. 5C), this trend was not statistically significant. For the deeper parts of the sand columns, changes in ^{13}C-TSC beyond 6 h were also not significant (Supplementary statistical analyses 4).

The average ^{13}C that ended up in the SIC pool was 2.3 μmol ^{13}C per core (Fig. 5F). This is less than 1% of the amount of ^{13}C incorporated into the TSC pool, indicating that almost all of the 0.3 mmol ^{13}C per core incorporated into the TSC pool ended up in the organic fraction (SOC) (Fig. 5I). Similar to TSC, variability in the amounts of ^{13}C-SIC observed at time points beyond 6 h was not significant, but the concentration of ^{13}C-SOC that ended up in the schmutzdecke was significantly higher than in deeper layers (Supplementary statistical analyses 5).

Trends in the isotopic composition of bacterial lipids reflected those observed for TSC, with the weighted average of $\delta^{13}C$-PLFA values increasing to around 400‰ during the first 6 h and then remaining at similarly high levels (400–700‰) until the end of the experiment (Fig. 6A). Significant differences among depths in the sand column, or trends over time, could not be resolved due to a limited number of replicate measurements. However, we did detect a higher concentration of ^{13}C taken up by the microbial biomass in the schmutzdecke in comparison to deeper layers, caused by the higher PLFA concentration, i.e. biomass, in this layer (Fig. 6B). Combining the $\delta^{13}C$-PLFA values with the time-averaged bacterial biomass derived from the PLFA content in five replicate cores (13.6 mmol C core^{-1}), the average amount of ^{13}C

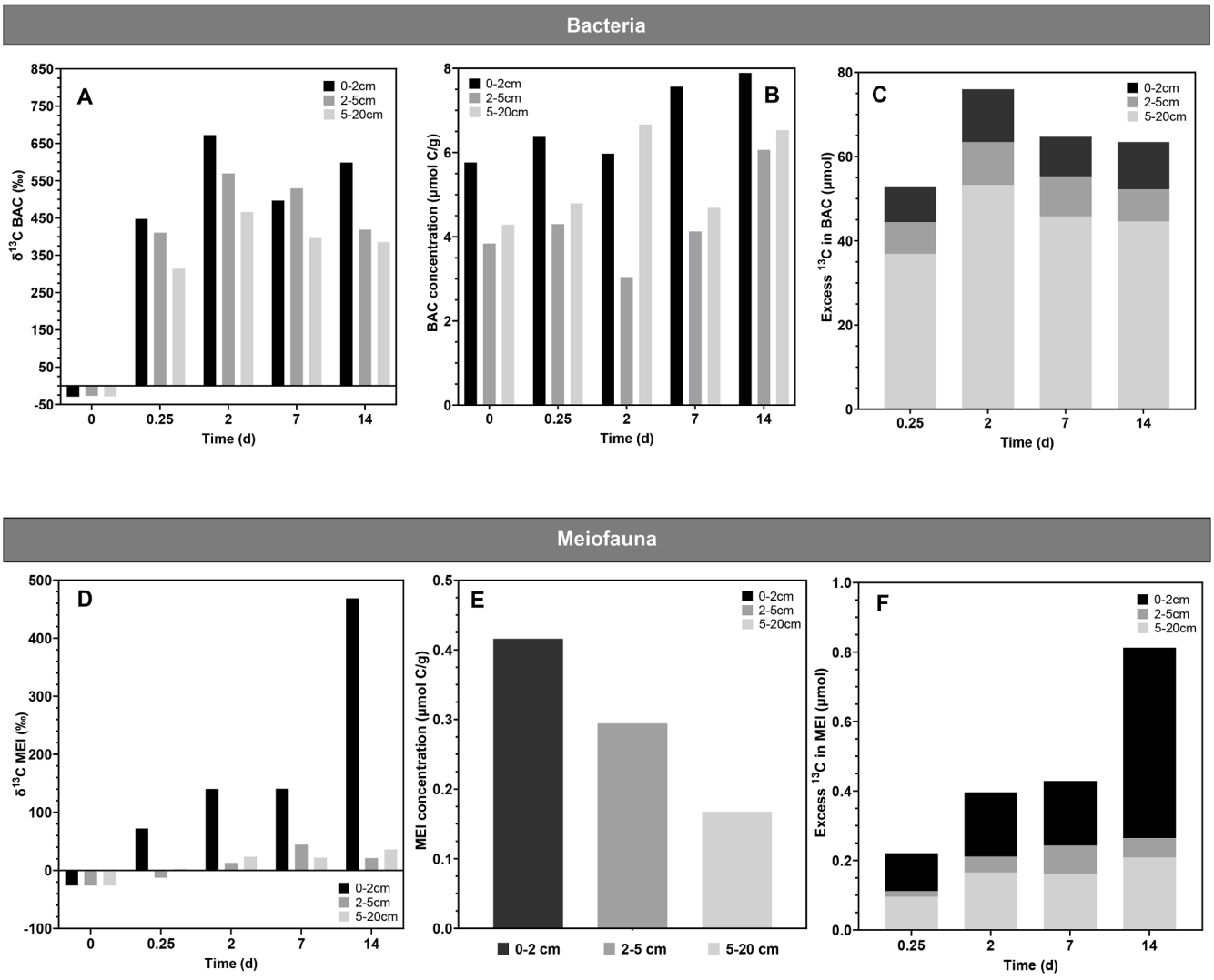

Fig. 6. Dynamics of specific biological carbon pools in the cores during the stable isotope labeling experiment. (A) Weighted averages of $\delta^{13}C$ in bacterial PLFAs. (B) Bacterial carbon concentrations, derived from the measured concentrations of PLFAs based on a conversion factor by Leckie et al. (2004). (C) Calculated amounts of excess ^{13}C incorporated into the bacterial pool. (D) Weighted averages of $\delta^{13}C$ measured in meiofauna (MEI). (E) Average carbon concentrations in the meiofaunal pool. (F) Calculated amounts of excess ^{13}C incorporated into the pool of meiofauna.

taken up by bacteria was around 0.066 ± 0.004 mmol ^{13}C per core (Fig. 6C). This amount accounts for about 22% of the estimated ^{13}C incorporated into the SOC pool. Using the alternative PLFA to bacterial biomass conversion factor based on Middelburg et al. (2000) provided comparable results, with the average amount of ^{13}C taken up by bacteria being around 0.073 ± 0.005 mmol ^{13}C per core (Supplementary Fig. S6).

For the meiofauna pool, $\delta^{13}C$ values increased during the initial 6 h of the SIL experiment, indicative of a direct ^{13}C-glucose uptake by the meiofauna (Fig. 6D). The $\delta^{13}C$ values trends increased over time with variations among depths in the sand column. In the schmutzdecke, the values steadily increased, reaching maximum values of around 470‰, and in deeper layers, the maximum was around 40‰. Due to a limited number of replicate measurements and high variability in the data, we could not test for significant differences in the $\delta^{13}C$ values observed over time after 6 h. To estimate the amount of ^{13}C incorporated into meiofauna, we therefore combined the $\delta^{13}C$ values with the time-averaged C content for the total meiofauna (Fig. 6E) and summed the contributions across all layers and all meiofaunal groups. The estimated values of 0.8 μmol ^{13}C in meiofauna per core (Fig. 6F) were at least 100-fold lower than the amount of ^{13}C assimilated by bacteria. The detailed results concerning individual meiofaunal species will be presented in a separate publication.

3.3. Effect of decalcification and washing

For sand samples collected during the SIL experiment, the standard decalcification treatment and washing with Milli-Q water had contrasting effects on the C and ^{13}C contents. On the one hand, the standard decalcification treatment decreased the carbon content on average by about 51% in the schmutzdecke and 45% in the sand bed (Fig. 7A), while the corresponding $\delta^{13}C$ values increased on average by 17‰ and 5‰, respectively (Fig. 7B). These results are consistent with those derived from independent analyses of the sand samples collected during the SIL experiment, which showed that the TSC pool contains a relatively large fraction of SIC (Supplementary Fig. S2) with $\delta^{13}C$ values ranging between 0–1.5‰ (Fig. 5D), and so the removal of such a pool should lead to an increase in the $\delta^{13}C$ value of the remaining carbon.

In contrast, washing with Milli-Q water did not decrease the carbon content in the samples, but it did lead to a notable decrease in the $\delta^{13}C$ values on average by 17‰. This decrease translates to a reduction in the solid-bound ^{13}C content and implies that the TSC pool contained a small but highly ^{13}C enriched fraction that could relatively easily be washed out by Milli-Q water.

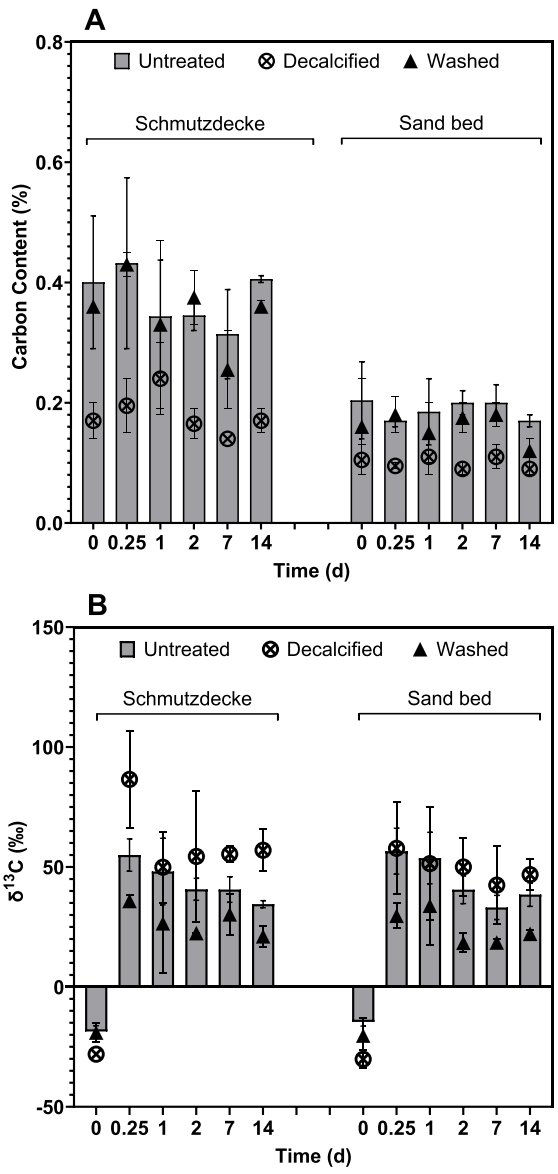

Fig. 7. Effects of sample preparation on the concentration (A) and isotopic composition (B) of the total solid carbon pool in sediment samples collected at the end of the stable isotope labeling experiment. The effects are shown separately for the schmutzdecke (0–2 cm) and the underlying sand layer (2–5 cm). `Untreated' refers to unaltered samples, `decalcified' refers to samples treated with 1M HCl, and `washed' refers to samples washed with MilliQ water (see Supplementary Methods S1 for further details). Error bars represent the range based on duplicate cores.

4. Discussion

In the Netherlands, slow sand filtration (SSF) is used as one of the last steps in the process of drinking water production. Its main purpose is to remove organic matter that has not been removed during the previous water treatment steps and thus ensure that the effluent water meets the required quality and safety standards (van der Kooij et al., 2017). In general, two classes of organic matter are relevant in the context of SSF: dissolved organic carbon (DOC), for which the easily assimilable organic carbon (AOC) is of key concern, and particulate organic carbon (POC), which includes components such as detritus and bacteria (Collins et al., 1992; Hijnen et al., 2004; Zheng et al., 2010). Organic matter removal in SSF is done through a combination of physical and biological processes (Weber-Shirk and Dick, 1997a, 1997b). This study aimed to explore the utility of stable isotopes for estimating the contribution of the biological activity (uptake and mineralization) in the removal of DOC, including AOC, in an operational slow sand filter.

4.1. Approaches based on concentration measurements

One way to estimate the role of biological activity in the removal of DOC is by quantifying the DOC fluxes in the influent and effluent waters of a slow sand filter and comparing their difference to the build-up of solid organic carbon (SOC) in the sand column. Our measurements revealed that the difference between the influent and effluent DOC concentrations was similar among the four sampling events (with an average of 0.049 mmol L^{-1}), although the concentrations themselves varied considerably (by about 40%; Table 1). Assuming that the water flow velocity of the studied full-scale filter is constant (0.35 m h^{-1}; Supplementary Table S1), this concentration difference translates to an organic carbon retention rate of about 61 mol C m^{-2} over a 6 month period. When measuring the SOC content in the sand column, which was done 6 months after the schmutzdecke had been cleaned, we found that about 32 mol C m^{-2} was present in the top 20 cm, out of which about 6.5 mol C m^{-2} was in the schmutzdecke (top 2 cm). Furthermore, TSC concentration was about 1.8-fold higher in the schmutzdecke than in

deeper layers. Thus, assuming that DOC removal occurred mainly in the most active layer, the schmutzdecke, which is a common assumption in SSF utilities and studies (Chen et al., 2021; Maurya et al., 2020; Ranjan and Prem, 2018), these data would indicate that up to 10% of the DOC removed over the 6-month period was retained in the developing schmutzdecke while the remaining 90% was mineralized. However, if DOC removal also occurred in deeper layers, as observed in previous studies on mature filters (Chan et al., 2018; Trikannad et al., 2024), the relative contribution of mineralization would be substantially lower. How much lower cannot be, however, presently resolved due to the lack of more detailed (historical) information about the SOC content in the studied filter and the corresponding influent and effluent DOC concentrations. Regular monitoring of these parameters over longer time scales and throughout the entire sand column could be a strategy to alleviate this limitation.

Another approach to estimate the contribution of mineralization to DOC removal is by measuring the increase in DIC concentrations between the effluent and influent. Indeed, the difference in DIC concentrations multiplied with the flow velocity directly yields the areal rate of mineralization (Worrall et al., 2005), if contributions of processes such as CO_2 stripping, carbonate precipitation, or dissolution can be neglected. Our measurements showed, however, that the DIC concentrations were more than one order of magnitude higher than those of DOC (Table 1), implying that high-precision DIC measurements (Su et al., 2019) would be required to resolve the relatively small differences in DIC concentrations (<0.04 mmol L^{-1}) expected to result from the observed differences in DOC concentrations.

4.2. Approaches based on measurements of natural isotopic composition

Our data suggest that DOC retention and removal in a slow sand filter could potentially be estimated by quantifying the natural isotopic composition of relevant carbon pools. With respect to DOC retention, we observed a vertical gradient in the $\delta^{13}C$ values of the total solid carbon (TSC) pool, increasing from about −19‰ in the schmutzdecke to −15‰ in deeper layers, reflecting a larger enrichment in ^{13}C with depth (Table 2). Interestingly, this gradient could be explained by assuming that the TSC pool is a mixture of solid-bound inorganic carbon (SIC, $\delta^{13}C \approx 0$‰) and SOC with the same isotopic composition as the influent DOC ($\delta^{13}C \approx -26$‰), with the mixing ratios consistent with the observed SOC:SIC ratios, which decreased from about 2:1 in the schmutzdecke to about 1:1 in deeper layers (Supplementary Fig. S2). This agreement points to physical processes (e.g., adsorption or straining) or biological uptake as key mechanisms of DOC retention in the sand column (Boström et al., 2007). It also illustrates that although the concentration of retained DOC is higher in the schmutzdecke, deeper sand layers are also important (Chan et al., 2018; Trikannad et al., 2024), even more so when considering the amount of organic carbon retained per unit area. Finally, the agreement suggests that DOC retention in the sand filter could possibly be estimated through monitoring the spatial-temporal variation in the $\delta^{13}C$ values of the TSC pool.

With respect to DOC removal, we consistently observed higher $\delta^{13}C$-DOC and lower $\delta^{13}C$-DIC values in the effluent compared with the influent (Table 1). These results are consistent with trends expected from the effects of kinetic isotope fractionation associated with organic matter mineralization (e.g., by aerobic respiration), where ^{12}C is preferentially released into the inorganic pool while the remaining organic pool becomes progressively enriched in ^{13}C (Wang et al., 2015). However, by applying a simple Rayleigh distillation model and assuming one set of kinetic fractionation factors for relevant processes including mineralization, adsorption, and uptake, we could not consistently reproduce the observed differences in the concentrations and $\delta^{13}C$ values for the effluent and influent DOC and DIC pools (see Supplementary modeling for details). These difficulties could be related to insufficient quality of our measurements or due to the DOC pool being comprised of constituents with a range of isotopic signatures, adsorption affinities, and labilities. Indeed, $\delta^{13}C$ values in DOC can change depending on the extent of adsorption (Kaiser et al., 2001) or due to a preferential uptake or mineralization of components in the complex DOC pool with a range of isotopic signatures (Vogt et al., 2016). Hence, isotope analyses of the DOC and DIC pools could help determine the contribution of microbial degradation to DOC removal, but the distribution of $\delta^{13}C$ values among the constituents comprising the influent and effluent DOC pools, as well as the isotope fractionation effects of the relevant processes within the sand column, need to be constrained first in dedicated measurements and experiments.

4.3. Approach based on stable isotope labeling

Our SIL experiment used ^{13}C-glucose as a proxy for easily degradable carbon. On the one hand, we recognize that glucose and its removal are not representative of all bioavailable organic compounds and their removal rates (Hammes et al., 2006). Indeed, uptake rates of low molecular weight substrates are diverse (Amon and Benner, 1996), and for instance, in soils, they can differ by an order of magnitude (Gunina et al., 2017). On the other hand, glucose removal can still be used as a valuable indicator of the biological community's potential to eliminate easily biodegradable organic compounds. Furthermore, monitoring the fate of glucose-derived ^{13}C can enhance our understanding of the mechanisms involved in the transformations of easily biodegradable organic compounds within the studied slow sand filter, as discussed in the following.

The rapid decrease in the concentration of glucose during the initial ~6 h of the experiment (Fig. 3A) reflects the capacity of the studied sand filter to remove easily degradable organic compounds via biological processes. For a sand column height of 20 cm, glucose removal occurred at a rate of about 14 mmol C m^{-2} h^{-1}, which by far exceeds the AOC loading of the studied sand filter (about 0.78 mmol C m^{-2} h^{-1}, estimated based on the influent AOC concentrations and flow rates; Tables 1 and Supplementary Table S1). Furthermore, the rate of glucose removal was independent of glucose concentrations in the investigated concentration range. Assuming that glucose removal follows Michaelis-Menten kinetics, this observed zero-order behavior suggests that, at the tested glucose concentrations, the removal rate was approaching the maximum rate (v_{max}) (Michaelis et al., 2011).

The initial removal of ^{13}C-glucose was accompanied by a notable increase in $\delta^{13}C$ values in the SOC and DIC pools, showing the importance of biological activity (through uptake and respiration) in the removal of the added glucose. Based on the amounts of excess ^{13}C accumulated in the SOC and DIC pools during the initial 6 h of the experiment, the estimated rate of glucose uptake was about 14 mmol ^{13}C m^{-2} h^{-1}, while the rate of glucose mineralization accompanying this uptake was about 1.7 mmol ^{13}C m^{-2} h^{-1}. These estimates indicate that about 47±5% of the added ^{13}C-glucose was taken up by the organisms in the sand column, while approximately 12% was mineralized into DIC as a direct consequence of this uptake. However, these values do not add up to 100%, indicating that a substantial fraction of the added ^{13}C tracer could not be accounted for (see below for possible reasons). Nevertheless, these data show that as long as glucose was available, its removal was dominated by biological uptake over mineralization.

A comparison between the amounts of excess ^{13}C recovered in the pools of TSC and bacterial biomass suggests that, during the initial 6 h of the experiment, a major part of the glucose taken up by the bacteria was retained in the form of storage compounds or carbon reserves rather than used for growth (e.g., by synthesizing structural biomass). While the amount of excess ^{13}C estimated for the bacterial biomass was around 0.07 mmol ^{13}C per core, the amount estimated for the TSC pool was about 4-fold greater (Figs. 5C and 6C). Although the $\delta^{13}C$ values in the meiofauna, which are part of the TSC pool, did increase after 6 h of incubation, the corresponding amount of excess ^{13}C was insufficient (<1 μmol ^{13}C) to explain this discrepancy. A possible reason for this discrepancy could be that the conversion factors of Leckie et al. (2004) and Middelburg et al. (2000), which we applied to estimate bacterial

biomass from the detected amounts of bacterial fatty acids, were not representative of the bacterial community in the studied sand column. Another possibility is that our measurements did not cover all bacterial PLFAs, or that excess ^{13}C derived from the measured values of $\delta^{13}C$-PLFA was not representative of all bacterial carbon synthesized during the initial 6 h (Evrard et al., 2010). A more likely explanation is, however, that bacteria allocated a fraction of the taken up ^{13}C-glucose to build up their carbon or energy reserves (van Loosdrecht et al., 1997), such as in the form of a carbon-rich energy storage compound glycogen (Sekar et al., 2020; Wang et al., 2020; Wang and Wise, 2011). Bacteria can accumulate more than 50% of their biomass in the form of glycogen (Levine et al., 1953). In our columns, we estimate the total bacterial biomass content to be 13 mmol C (Fig. 2). As the difference between the incorporation of ^{13}C in TSC and bacterial biomass is only 0.23 mmol C and assuming that biomass is typically 50% carbon (Houghton et al., 2009), carbon storage would be sufficient to explain the observed discrepancy. Another possible explanation is that glucose attached to or became incorporated into EPS, which can also act as a carbon reserve (Costa et al., 2018; Wingender et al., 1999). The incorporation of ^{13}C into storage compounds or EPS is consistent with the observed decrease in $\delta^{13}C$-TSC upon washing with Milli-Q water (Fig. 7B). The washing process may have led to the removal of EPS, along with the associated ^{13}C, and the detachment of bacteria embedded within the EPS. Consequently, the unprotected bacteria may have released water-soluble storage compounds, such as glycogen, which could further explain the selective loss of ^{13}C from the TSC pool upon washing. Adsorption of glucose to the sand could also offer a potential explanation for the observed excess ^{13}C in the TSC pool compared to the estimated amounts in microbial biomass. However, complementary glucose adsorption experiments conducted with both autoclaved and bioactive sand (Supplementary Methods S6; Supplementary Fig. S7) demonstrated that the contribution of abiotic processes to glucose removal was negligible.

With respect to meiofauna, our SIL experiment provided only limited insights into their role in the studied slow sand filter. The rapid increase in meiofaunal $\delta^{13}C$ during the initial 6 h indicates that they can directly utilize the added glucose, while the gradual increase in $\delta^{13}C$ observed subsequently was likely due to the uptake of ^{13}C previously assimilated by bacteria (van Oevelen et al., 2006a, 2006b). This uptake could occur via direct predation or ingestion of dead and labile material of bacterial origin (Schratzberger and Ingels, 2018). Overall, the slow increase in meiofaunal $\delta^{13}C$ suggests that the SSF's heterotrophic bacterial community plays only a minor role in the meiofauna's diet. Furthermore, the amount of excess ^{13}C in meiofauna after 14 days (Fig. 6F) was at least 100-fold smaller compared to that in bacteria (Fig. 6C), indicating a minor role of meiofauna in the label uptake during the experiment. However, meiofauna have a broad diet (Majdi et al., 2020), including detrital material, which can pass the previous steps of drinking water production and become retained in the slow sand filter. Hence, it is possible that the net effect of meiofauna activity is to support microbial growth by digesting detrital organic material and making it more accessible to bacteria (Coull, 2009). For instance, earthworms can play a vital role in sand filters, as their activity facilitates the degradation of complex and recalcitrant organic matter and mitigates clogging (Oh et al., 2018; Wang et al., 2010; Wubbels et al., 2014).

$\delta^{13}C$ values in the TSC pool as well as in the bacterial and meiofaunal biomass measured 6 h after label addition increased across the different depths in the experimental cores (Figs. 5A, 6A, D), showing that the biological removal of easily degradable organic carbon is not limited to the schmutzdecke but extends at least 20 cm deep into the slow sand filter. Because the concentration of organic carbon in the schmutzdecke was about 2-fold higher than in the deeper layers of the sand columns, the concentration of the taken up ^{13}C-glucose was correspondingly higher as well. However, as the schmutzdecke only comprised 10% of the height of the experimental sand columns, the absolute amount of glucose taken up in the schmutzdecke only accounted for less than 20% of the glucose uptake per 20 cm sand column. These findings are consistent with earlier studies suggesting that biological activity can extend as deep as 40 cm into the sand bed (Ellis and Aydin, 1995; Huisman and Wood, 1974). They also support observations that DOC reduction in the deeper layers of slow sand filters indicates the microbial community's ability to degrade biodegradable dissolved organic carbon (BDOC) throughout the filter's depth (Trikannad et al., 2024). Taken together, our results and previous research emphasize the critical role of biological activity not only in the schmutzdecke but also in the deeper layers of slow sand filters.

An unexpected finding of our SIL experiment was the notably long residence time of ^{13}C in the experimental cores (much longer than 14 days). As a result, we were unable to estimate the mineralization rate of the ^{13}C-glucose after it had been taken up by the bacterial community. One way to constrain this rate would be by following the decline in the amount of excess ^{13}C in the organic carbon pools (SOC and PLFA). However, although the excess ^{13}C in these pools did vary among the cores sacrificed at different time points (Figs. 5I, 6C), the variation reflected mainly inter-core differences and showed no notable change over time. Another approach to estimate the mineralization rate of the taken up glucose would be by measuring the increase in excess ^{13}C in the DIC pool. However, these values gradually decreased after 6 h of incubation rather than increased (Fig. 4). We attribute this decrease to isotope exchange with atmospheric CO_2 through the tubing used in our experiments, which was apparently too permeable (CO_2 permeability coefficient was $1.89\ \frac{(cm^3 \cdot mm)}{(cm^2 \cdot s \cdot Pa) \times 10^{-10}}$) to keep the ^{13}C content in the system constant during the entire experiment. We rule out carbonate precipitation as a sink for ^{13}C-DIC because the amount of excess ^{13}C accumulated in the SIC pool was too small to explain this trend. Another option is that the observed decrease in $\delta^{13}C$-DIC resulted from a dilution of the ^{13}C-DIC pool by the excess production of ^{12}C-DIC associated with the mineralization of SOC or dissolution of SIC in the sand column, which is possible because both SOC and SIC had lower $\delta^{13}C$ values than the DIC pool between days 1 and 14. However, the estimated excess ^{12}C-DIC production required to account for the observed decrease in $\delta^{13}C$-DIC over the period of 14 days would be about 12–15 mmol $^{12}C\ L^{-1}$, which is sufficiently high to be detectable as an increase in DIC concentrations within the experimental cores. Since such a substantial increase was not observed during our labeling experiment, this second option can also be ruled out. This decrease in respiration may also be attributed to the recirculation of water, as each pass through the sand likely depleted other essential nutrients required for mineralization. Irrespective of the precise mechanism behind the long-term decrease in $\delta^{13}C$-DIC, it is certain that once the added glucose was taken up, mineralization of this glucose-derived carbon occurred at a much lower rate than glucose mineralization directly associated with glucose uptake (i.e., during the initial 6 h).

The design of future isotope labeling experiments needs to consider specific circumstances that were unforeseen in this study. First, tubing with a much lower permeability towards CO_2 gas needs to be used to minimize isotope exchange with atmospheric CO_2. This precaution will make it possible to estimate the possibly very slow mineralization of the added isotopically labeled probe thus reconstruct a more accurate carbon balance within the sand core. Second, the ^{13}C-labelled substrate should reflect more accurately the conditions typically encountered in SSF (possibly acetate). Furthermore, the label should be added at concentrations sufficiently high to maximize labeling across the microbial community while avoiding excessive concentrations that could result in unwarranted or undesirable physiological responses of the organisms involved (e.g., accumulation and long-term retention of storage reserves). Overall, due to generally low biological activity in the filter, the entire experiment needs to be done over longer time scales to better constrain the fate of assimilated carbon and its use within the food web.

5. Conclusions

Stable isotopes are a valuable tool for elucidating the role of biological activity in the removal of organic carbon during slow sand filtration. The contribution of biological uptake and respiration can be estimated based on measurements of the concentration and natural isotopic composition of DOC and DIC in the influent and effluent waters. For this approach to be practical, regular monitoring of these parameters and with sufficient precision, is required. Additionally, dedicated experiments targeting kinetic isotope fractionation effects of the relevant processes within the sand filter are necessary to aid quantitative interpretation of the isotope data. Another promising approach involves stable isotope labeling (SIL) experiments using ^{13}C-labeled assimilable carbon source as a tracer. Findings from the SIL experiment reveal that about 12% of the glucose added was directly mineralized during uptake, while the majority was taken up and used for growth or allocated into storage reserves. The uptake of glucose was dominated by bacteria. In contrast, meiofauna only accounted for a small fraction of the glucose uptake. Moreover, the biological activity extends well beyond the schmutzdecke layer, indicating that lengthy ripening periods may not be required to restore filter efficiency after routine cleaning. Instead, the biological activity in the deeper layers of the filter is likely sufficient to sustain effective organic carbon removal. For future application, SIL could be used to compare the potential removal efficiencies of easily degradable organic carbon in filters operating under different conditions, monitor the removal efficiency in a maturing filter, or contrast the removal efficiencies in the schmutzdecke versus deeper filter layers.

CRediT authorship contribution statement

Bayan Khojah: Writing – original draft, Visualization, Validation, Methodology, Investigation, Formal analysis, Conceptualization. **Salima Sadeghi:** Conceptualization, Methodology, Investigation. **Lubos Polerecky:** Writing – review & editing, Validation, Supervision, Methodology, Funding acquisition, Formal analysis, Conceptualization. **Jack J. Middelburg:** Writing – review & editing, Supervision, Methodology, Funding acquisition, Conceptualization. **Dick van Oevelen:** Writing – review & editing, Methodology, Funding acquisition, Conceptualization. **Marcel T.J. van der Meer:** Writing – review & editing, Methodology, Funding acquisition, Conceptualization. **Thilo Behrends:** Writing – review & editing, Validation, Supervision, Project administration, Methodology, Funding acquisition, Formal analysis, Conceptualization.

Declaration of competing interest

The authors declare the following financial interests/personal relationships which may be considered as potential competing interests:

Thilo Behrends reports financial support was provided by Dutch Research Council. If there are other authors, they declare that they have no known competing financial interests or personal relationships that could have appeared to influence the work reported in this paper.

Acknowledgment

This research was funded by the Netherlands Organization for Scientific Research (NWO) through the Dunea–Vitens: Sand Filtration partnership program (grant 17838). We are grateful to Fenna Philipse from Waternet for her assistance in obtaining the sand columns and water samples. Special thanks to the laboratory staff at Utrecht University, including A. van Dijk, D.D. Eefting, J.J. van Tongeren, and T.H. H. Claessen, for their work on the chemical analysis. We also appreciate J.P. de Witte for designing and fabricating the experimental columns and T. Marcus for the graphical design. We extend our gratitude to S. Bouillon and Y. Stroobandt from KU Leuven for δ^{13}C-DOC analysis. Lastly, we acknowledge the contributions of our students, I.E. Frederiks, D. Bouland, and M.G. van Reenen, for their assistance with meiofauna analysis.

Supplementary materials

Supplementary material associated with this article can be found, in the online version, at doi:10.1016/j.watres.2025.123249.

Data availability

Data will be made available on request.

References

Amon, R.M.W., Benner, R., 1996. Bacterial utilization of different size classes of dissolved organic matter. Limnol. Oceanogr. 41 (1), 41–51.
Bai, X., Dinkla, I.J.T., Muyzer, G., 2023. Shedding light on the total and active core microbiomes in slow sand filters for drinking water production. Water. Res. 243, 120404.
Bergamino, L., Lercari, D., Defeo, O., 2011. Food web structure of sandy beaches: temporal and spatial variation using stable isotope analysis. Estuar. Coast. Shelf. Sci. 91 (4), 536–543.
Bichai, F., Hijnen, W., Baars, E., Rosielle, M., Dullemont, Y., Barbeau, B., 2011. Preliminary study on the occurrence and risk arising from bacteria internalized in zooplankton in drinking water. Water Sci. Technol. 63 (1), 108–114.
Bomo, A.M., Stevik, T.K., Hovi, I., Hanssen, J.F., 2004. Bacterial removal and protozoan grazing in biological sand filters. J. Environ. Qual. 33 (3), 1041–1047.
Boschker, H.T.S., Middelburg, J.J., 2002. Stable isotopes and biomarkers in microbial ecology. FEMS Microbiol. Ecol. 40 (2), 85–95.
Boström, B., Comstedt, D., Ekblad, A., 2007. Isotope fractionation and C-13 enrichment in soil profiles during the decomposition of soil organic matter. Oecologia 153, 89–98.
Bridgeman, J., Gulliver, P., Roe, J., Baker, A., 2014. Carbon isotopic characterisation of dissolved organic matter during water treatment. Water. Res. 48, 119–125.
Campos, L.C., Su, M.F., Graham, N.J., Smith, S.R., 2002. Biomass development in slow sand filters. Water. Res. 36 (18), 4543–4551.
Chan, S., Pullerits, K., Riechelmann, J., Persson, K.M., Radstrom, P., Paul, C.J., 2018. Monitoring biofilm function in new and matured full-scale slow sand filters using flow cytometric histogram image comparison (CHIC). Water. Res. 138, 27–36.
Chen, L., Zhai, Y., van der Mark, E., Liu, G., van der Meer, W., Medema, G., 2021. Microbial community assembly and metabolic function in top layers of slow sand filters for drinking water production. J. Clean. Prod. 294, 126342.
Collins, M., Eighmy, T.T., Jr, J., Spanos, S., 1992. Removing natural organic matter by conventional slow sand filtration. J. Am. Water Works Assoc. 84, 80–90.
Costa, O.Y.A., Raaijmakers, J.M., Kuramae, E.E., 2018. Microbial extracellular polymeric substances: ecological function and impact on soil aggregation. Front. Microbiol. 9.
Coull, B., 2009. Role of meiofauna in estuarine soft-bottom habits. Aust. J. Ecol. 24, 327–343.
Ellis, K.V., Aydin, M.E., 1995. Penetration of solids and biological activity into slow sand filters. Water. Res. 29 (5), 1333–1341.
Evrard, V., Soetaert, K., Heip, C.H.R., Huettel, M., Xenopoulos, M.A., Middelburg, J.J., 2010. Carbon and nitrogen flows through the benthic food web of a photic subtidal sandy sediment. Mar. Ecol. Prog. Ser. 416, 1–16.
Fang, J., Barcelona, M.J., Krishnamurthy, R.V., Atekwana, E.A., 2000. Stable carbon isotope biogeochemistry of a shallow sand aquifer contaminated with fuel hydrocarbons. Appl. Geochem. 15 (2), 157–169.
Ghashghaie, J., Badeck, F.-W., Lanigan, G., Nogués, S., Tcherkez, G., Deléens, E., Cornic, G., Griffiths, H., 2003. Carbon isotope fractionation during dark respiration and photorespiration in C3 plants. Phytochem. Rev. 2, 145–161.
Glibert, P.M., Middelburg, J.J., McClelland, J.W., Jake Vander Zanden, M., 2018. Stable isotope tracers: enriching our perspectives and questions on sources, fates, rates, and pathways of major elements in aquatic systems. Limnol. Oceanogr. 64 (3), 950–981.
Gunina, A., Smith, A.R., Kuzyakov, Y., Jones, D.L., 2017. Microbial uptake and utilization of low molecular weight organic substrates in soil depend on carbon oxidation state. Biogeochemistry 133 (1), 89–100.
Haig, S.J., Collins, G., Davies, R., Dorea, C., Quince, C., 2011. Biological aspects of slow sand filtration: past, present and future. Water Sci. Technol. 11, 468–472.
Haig, S.J., Quince, C., Davies, R.L., Dorea, C.C., Collins, G., 2015a. The relationship between microbial community evenness and function in slow sand filters. mBio 6 (5), e00729, 00715.
Haig, S.J., Schirmer, M., D'Amore, R., Gibbs, J., Davies, R., Collins, G., Quince, C., 2015b. Stable-isotope probing and metagenomics reveal predation by protozoa drives E. coli removal in slow sand filters. ISMe J. 9, 797–808.
Hammes, F., Salhi, E., Köster, O., Kaiser, H.-P., Egli, T., von Gunten, U, 2006. Mechanistic and kinetic evaluation of organic disinfection by-product and assimilable organic carbon (AOC) formation during the ozonation of drinking water. Water. Res. 40 (12), 2275–2286.
Hammes, F., Velten, S., Egli, T., Juhna, T., 2011. Comprehensive Biotechnology, Second Edition. Academic Press, Burlington, pp. 517–530. Moo-Young, M. (ed).
Hendel, B., Marxsen, J., Fiebig, D., Preuß, G., 2001. Extracellular enzyme activities during slow sand filtration in a water recharge plant. Water. Res. 35 (10), 2484–2488.

Henniger, G., Mascaro Jr., L., 1985. Enzymatic-ultraviolet determination of glucose and fructose in wine: collaborative study. J. Assoc. Off. Anal. Chem. 68 (5), 1021–1024.
Hidayah, E.N., Chou, Y.-C., Yeh, H.-H., 2018. Characterization and removal of natural organic matter from slow sand filter effluent followed by alum coagulation. Appl. Water. Sci. 8 (1), 3.
Hijnen, W.A.M., Schijven, J.F., Bonné, P., Visser, A., Medema, G.J., 2004. Elimination of viruses, bacteria and protozoan oocysts by slow sand filtration. Water Sci. Technol. 50 (1), 147–154.
Houghton, R.A., Hall, F., Goetz, S.J., 2009. Importance of biomass in the global carbon cycle. J. Geophys. Res. Biogeosci. 114 (G2).
Huisman, L., Wood, W.E., 1974. Slow Sand Filtration. World Health Organization.
Kaiser, K., Guggenberger, G., Zech, W., 2001. Isotopic fractionation of dissolved organic carbon in shallow forest soils as affected by sorption. Eur. J. Soil. Sci. 52, 585–597.
Leckie, S.E., Prescott, C.E., Grayston, S.J., Neufeld, J.D., Mohn, W.W., 2004. Characterization of humus microbial communities in adjacent forest types that differ in nitrogen availability. Microb. Ecol. 48 (1), 29–40.
Lerch, T., Nunan, N., Dignac, M.-F., Chenu, C., Mariotti, A., 2011. Variations in microbial isotopic fractionation during soil organic matter decomposition. Biogeochemistry 106, 5–21.
Levine, S., Stevenson, H.J.R., Tabor, E.C., Bordner, R.H., Chambers, L.A., 1953. Glycogen of enteric bacteria. J. Bacteriol. 66 (6), 664–670.
Lloyd, B., 1973. The construction of a sand profile sampler: its use in the study of the Vorticella populations and the general interstitial microfauna of slow sand filters. Water. Res. 7 (7), 963–973.
Lubarsky, H., Fava, N., Freitas, B., Terin, U., Oliveira, M., Lamon, A., Pichel, N., Byrne, J., Sabogal Paz, L., Fernandez-Ibanez, P., 2022. Biological layer in household slow sand filters: characterization and evaluation of the impact on systems efficiency. Water. (Basel) 14 (7), 1078.
Majdi, N., Schmid-Araya, J.M., Traunspurger, W., 2020. Examining the diet of meiofauna: a critical review of methodologies. Hydrobiologia 847 (12), 2737–2754.
Maqbool, T., Cho, J., Shin, K.H., Hur, J., 2020. Using stable isotope labeling approach and two dimensional correlation spectroscopy to explore the turnover cycles of different carbon structures in extracellular polymeric substances. Water. Res. 170, 115355.
Maurya, A., Singh, M.K., Kumar, S., 2020. Waterborne Pathogens. Butterworth-Heinemann, pp. 123–141.
Michaelis, L., Menten, M.L., Johnson, K.A., Goody, R.S., 2011. The original Michaelis constant: translation of the 1913 Michaelis-Menten paper. Biochemistry 50 (39), 8264–8269.
Middelburg, J., Barranguet, C., Boschker, H., Herman, P., Moens, T., Heip, C., 2000. The fate of intertidal microphytobenthos: an in situ 13C labeling study. Limnol. Oceanogr. 45, 1224–1234.
Middelburg, J.J., 2014. Stable isotopes dissect aquatic food webs from the top to the bottom. Biogeosciences 11 (8), 2357–2371.
Miyatake, T., Moerdijk-Poortvliet, T.C.W., Stal, L.J., Boschker, H.T.S., 2014. Tracing carbon flow from microphytobenthos to major bacterial groups in an intertidal marine sediment by using an in situ 13C pulse-chase method. Limnol. Oceanogr. 59 (4), 1275–1287.
Monson, K.D., Hayes, J.M., 1982. Carbon isotopic fractionation in the biosynthesis of bacterial fatty acids. Ozonolysis of unsaturated fatty acids as a means of determining the intramolecular distribution of carbon isotopes. Geochim. Cosmochim. Acta 46 (2), 139–149.
Oh, S., Hammes, F., Liu, W.-T., 2018. Metagenomic characterization of biofilter microbial communities in a full-scale drinking water treatment plant. Water. Res. 128, 278–285.
Pinheiro, J.C., Bates, D.J. and R-core, A. 2021 Nlme: linear and nonlinear mixed effects models, pp. Available online at: https://svn.r-project.org/R-packages/trunk/nlme/. (accessed March 1, 2021).
Poberžnik, M., Leis, A., Lobnik, A., 2012. Use of a stable carbon isotope to assess the efficiency of a drinking water treatment method with CO2. Water Sci. Technol. 65 (6), 983–988.
Polerecky, L., Eichner, M., Masuda, T., Zavřel, T., Rabouille, S., Campbell, D.A., Halsey, K., 2021. Calculation and interpretation of substrate assimilation rates in microbial cells based on isotopic composition data obtained by nanoSIMS. Front. Microbiol. 12, 1–17.
R Core Team, 2024. R: A Language And Environment For Statistical Computing. R Foundation for Statistical Computing, Vienna, Austria. URL. https://www.R-project.org/.
Ranjan, P., Prem, M., 2018. Schmutzdecke- a filtration layer of slow sand filter. Int. J. Curr. Microbiol. Appl. Sci. 7, 637–645.
Schouten, S., Hopmans, E.C., Baas, M., Boumann, H., Standfest, S., Könneke, M., Stahl, D. A., Sinninghe Damsté, J.S., 2008. Intact membrane lipids of "Candidatus Nitrosopumilus maritimus," a cultivated representative of the cosmopolitan mesophilic group I Crenarchaeota. Appl. Environ. Microbiol. 74 (8), 2433–2440.
Schratzberger, M., Ingels, J., 2018. Meiofauna matters: the roles of meiofauna in benthic ecosystems. J. Exp. Mar. Biol. Ecol. 502, 12–25.
Seeger, E.M., Braeckevelt, M., Reiche, N., Müller, J.A., Kästner, M., 2016. Removal of pathogen indicators from secondary effluent using slow sand filtration: optimization approaches. Ecol. Eng. 95, 635–644.
Sekar, K., Linker, S.M., Nguyen, J., Grünhagen, A., Stocker, R., Sauer, U., 2020. Bacterial glycogen provides short-term benefits in changing environments. Appl. Environ. Microbiol. 86 (9), 1–12.
Somerfield, P.J., Warwick, R.M., 2013. Methods for the Study of Marine Benthos. Wiley-Blackwell, pp. 253–284.
Su, J., Cai, W.-J., Hussain, N., Brodeur, J., Chen, B., Huang, K., 2019. Simultaneous determination of dissolved inorganic carbon (DIC) concentration and stable isotope (δ13C-DIC) by cavity ring-down spectroscopy: application to study carbonate dynamics in the Chesapeake Bay. Mar. Chem. 215, 103689.
Teece, M., Fogel, M., Dollhopf, M., Nealson, K., 1999. Isotope fractionation during biosynthesis of fatty acids by a marine bacterium and implications for paleoenvironmental studies. Org. Geochem. 30, 1571–1579.
Trikannad, S.A., van Halem, D., Foppen, J.W., van der Hoek, J.P., 2023. The contribution of deeper layers in slow sand filters to pathogens removal. Water. Res. 237, 119994.
Trikannad, S.A.A., Valentina, van der Wielen, P.W.J.J., Smidt, H., van der Hoek, J.P., van Halem, D, 2024. Recovery of microbial biomass and purification performance after scraping of full-scale slow sand filters. J. Water. Process. Eng. 60, 105101.
Unger, M., Collins, M.R., 2008. Assessing Escherichia coli removal in the schmutzdecke of slow-rate biofilters. Am. Water Works Assoc. 100 (12), 60–73.
van der Kooij, D., 1992. Assimilable organic carbon as an indicator of bacterial regrowth. J. Am. Water Works Assoc. 84, 57–65.
van der Kooij, D., Veenendaal, H.R., van der Mark, E.J., Dignum, M., 2017. Assessment of the microbial growth potential of slow sand filtrate with the biomass production potential test in comparison with the assimilable organic carbon method. Water. Res. 125, 270–279.
van Loosdrecht, M.C.M., Pot, M.A., Heijnen, J.J., 1997. Importance of bacterial storage polymers in bioprocesses. Water Sci. Technol. 35 (1), 41–47.
van Oevelen, D., Middelburg, J., Soetaert, K., Moodley, L., 2006a. The fate of bacterial carbon in an intertidal sediment: modeling an in situ isotope tracer experiment. Limnol. Oceanogr. 51, 1302–1314.
van Oevelen, D., Moodley, L., Soetaert, K., Middelburg, J., 2006b. The trophic significance of bacterial carbon in a marine intertidal sediment: results of an in situ stable isotope labeling study. Limnol. Oceanogr. 51, 2349–2359.
Vogt, C., Dorer, C., Musat, F., Richnow, H.H., 2016. Multi-element isotope fractionation concepts to characterize the biodegradation of hydrocarbons - from enzymes to the environment. Curr. Opin. Biotechnol. 41, 90–98.
Wang, D.-B., Zhang, Z.-Y., Li, X.-M., Zheng, W., Ding, Y., Yang, B., Yang, Q., Zeng, T.-J., Cao, J.-B., Yue, X., Shen, T.-T., Zeng, G.-M., Deng, J.-H., He, X, 2010. Effects of earthworms on surface clogging characteristics of intermittent sand filters. Water Sci. Technol. 61 (11), 2881–2888.
Wang, G., Jia, Y., Li, W., 2015. Effects of environmental and biotic factors on carbon isotopic fractionation during decomposition of soil organic matter. Sci. Rep. 5 (1), 11043.
Wang, L., Wang, M., Wise, M.J., Liu, Q., Yang, T., Zhu, Z., Li, C., Tan, X., Tang, D., Wang, W., 2020. Recent progress in the structure of glycogen serving as a durable energy reserve in bacteria. World J. Microbiol. Biotechnol. 36 (1), 14.
Wang, L., Wise, M.J., 2011. Glycogen with short average chain length enhances bacterial durability. Naturwissenschaften 98 (9), 719–729.
Weber-Shirk, M.L., Chan, K.L., 2007. The role of aluminum in slow sand filtration. Water. Res. 41 (6), 1350–1354.
Weber-Shirk, M.L., Dick, R.I., 1997a. Biological mechanisms in slow sand filters. J. Am. Water Works Assoc. 89 (2), 72–83.
Weber-Shirk, M.L., Dick, R.I., 1997b. Physical—chemical mechanisms in slow sand filters. J. AWWA 89 (1), 87–100.
Webster, G., Watt, L.C., Rinna, J., Fry, J.C., Evershed, R.P., Parkes, R.J., Weightman, A.J., 2006. A comparison of stable-isotope probing of DNA and phospholipid fatty acids to study prokaryotic functional diversity in sulfate-reducing marine sediment enrichment slurries. Environ. Microbiol. 8 (9), 1575–1589.
Wingender, J., Neu, T., Flemming, H.-C., 1999. Microbial Extracellular Polymeric Substances. Springer.
Worrall, F., Burt, T., Adamson, J., 2005. Fluxes of dissolved carbon dioxide and inorganic carbon from an upland peat catchment: implications for soil respiration. Biogeochemistry 73 (3), 515–539.
Wubbels, G., Bruins, J., Bosman, M., Woerdt, D.V.d., 2014. The Functioning of Biological Slow Sand Filtration in Relation to the Presence and the Role of Annelids in the Schmutzdecke, in Nakamoto, N., Graham, N., Collins, M. R, and Gimbel, R. (Eds.) Progress in Slow Sand and Alternative Biofiltration Processes: Further Developments and Applications. IWA Publishing, pp. 103–109.
Zheng, X., Ernst, M., Jekel, M., 2010. Pilot-scale investigation on the removal of organic foulants in secondary effluent by slow sand filtration prior to ultrafiltration. Water Res. 44 (10), 3203–3213.